富山大学トリチウム科学センター研究報告 6 ：25—38，1986

論 文

黒鉛による水素同位体の捕獲と再放出
——鉄不純物の影響及び再結合係数——

芦 田 完・渡 辺 国 昭*

富山大学放射性同位元素総合実験室
*富山大学トリチウム科学センター
〒930 富山市五福3190番地

Capture and Thermal Release of Hydrogen Isotopes by／from Graphite
—— Effect of Iron Impurity Doped to Graphite Surface and Recombination Factors——

Kan ASHIDA and *Kuniaki WATANABE

RI Lab., Toyama University,
*Tritium Research Center, Toyama University,
Gofuku 3190, Toyama 930, Japan

(Received December 25, 1986)

Abstract

To know the effect of metallic impurities deposited over the graphite first wall of thermonuclear fusion devices on the trapping-detrapping processes of fuel particles, the desorption processes of hydrogen isotopes implanted into the graphite doped with iron (3at. %) was studied using XPS and TDS. Hydrogen isotope ions were implanted into a sample at room temperature with 5 keV using a conventional ion gun. An impurity modification phenomenon was found for the thermal desorption process. Namely, a new desorption peak (denoted as [Fe/C]-peak) appeared for the graphite doped with iron. The desorption mechanism for [Fe/C]-peak was explained by the

second order surface recombination of trapped hydrogen atoms. The rate constants were determined as

$$k(H_2) = (7\times10^{-4})\exp(-59\times10^{3}/RT)$$
$$k(D_2) = (4\times10^{-4})\exp(-59\times10^{3}/RT)$$
$$k(T_2) = \nu_d(T_2)\exp(-59\times10^{3}/RT)$$

where the frequency factor and activation energy are [1/molec · sec] and [cal/mol] unit, respectively. The recombination factor for hydrogen isotopes were estimated as

$$k_r(H_2) = (1.5\times10^{-15})\exp(-59\times10^{3}/RT)\ [\mathrm{cm^4/molec\cdot sec}]$$
$$k_r(D_2) = (9.6\times10^{-15})\exp(-59\times10^{3}/RT)$$
$$k_r(T_2) = \nu_d(T_2)\times(2.6\times10^{-12})\exp(-59\times10^{3}/RT)$$

It was concluded that the impurity modification on the trapping-detrapping process is due to the increase in electronic charge on carbon caused by the presence of iron dopant.

1 Introduction

The recycling, inventory and permeation of fuel particles in/through the first wall are important problems to confine high temperature plasma in thermonuclear fusion devices. These phenomena should also be taken into account from the viewpoint of the safe handling of tritium . To predict the behavior of fuel particle in the first wall, the mechanisms of trapping-detrapping processes of them in cadidate materials should be studied in detail.

Graphite or carbon is one of the candidate materials for the first wall owing to its low-Z, refractory nature and ease in fabrication. There is a number of investigations on the sputtering/erosion[1-5], recycling and inventory of hydrogen isotopes[6-9] for this material. We have also studied the trapping states and detrapping processes of three hydrogen isotopes to understand the fundamental processes of trapping-detrapping and isotope effect[10-12]. We have observed that the property of pyrolytic graphite is modified due to accumulation of radiation damage[13]. As a result, mechanisms and kinetic parameters in the trapping-detrapping processes are altered from those of the graphite without radiation damage.

In those investigations, however, attention has been paid only to pure graphite. On the other hand, it is reported that metallic impurities such as iron, nickel and chromium, amounting to $10^{16}-10^{18}$ atoms/cm^2, are deposited on the graphite limiter in tokamaks[14-17]. This calls for attention to the modification of graphite property owing to the presence of such impurities, because the trapping-detrapping processes of fuel particles will be altered from those of pure graphite.

From this viewpoint, we studied the effect of iron impurity on the desorption processes of hydrgen isotopes implanted into graphite by means of X-ray photoelectron spectroscopy (XPS) and mass analyzed thermal desorption spectroscopy (TDS).

2 Experimental

The samples used were a graphite sheet (Papyex, 10×20×0.3mm) and one whose sub-surface region was doped with iron. The latter was prepared with sputter deposition of iron and subsequent vacuum annealing. That is, the graphite sheet was coated with iron by use of a conventional sputtering apparatus (ULVAC SBR-1104), operated with argon plasma at 200W. The thickness of the iron film was 500Å. Subsequently, this sample was mounted to a sample holder of an UHV apparatus equipped with XPS and SIMS (secondary ion mass spectroscopy) optics. It was annealed *in vacuo* at a temperature ranging from room temperature to 1000℃ for 10 minutes and cooled down to room temperature. The temperature of the sample was measured with a Pt-Pt/Rh (13%) thermocouple spot-welded to a tantalum sheet attached to the sample.

A double pass cylindrical mirror was used as the energy analyzer of photoelectrons. The probe was Mg-K_α line (1253.6eV). The energy of photoelectrons was calibrated against $Au4f_{7/2}$ peak (83.7eV)[18]. In the present study, a given XPS peak was reproduced within 0.1 eV errors. The details of the other experimental conditions and procedures have been described elsewhere[10-12].

After the sample surface was doped with iron (this sample is denoted as Fe/Papyex), with vacuum heating at 1000℃, it was used as a sample for thermal desorption measurements. The thermal desorption spectra were also measured for pure graphite (it is denoted as Papyex) to see the effect of the iron dopant on the desorption process.

To measure the TDSs of hydrogen isotopes, the sample was mounted to another UHV apparatus with a B-A gauge, quadrupole mass spectrometer and conventional ion gun (PHI 04-191). This apparatus was designed for use of tritium up to 5Ci/run. The B-A gauge and quadrupole mass spectrometer had been calibrated against hydrogen isotopes[19]. The details of the TDS measurements have been described elsewhere[10-12].

3 Results

3 - 1 Sample characterization

Fig. 1. shows the change in the wide range XPS spectra of iron coated graphite with annealing temperature. Before vacuum heating, the sample was covered with impurities such as carbon and oxygen. Hence, the Fe2p peak was weak. Above 500℃, the Cls and Fe2p peak became predominant, while the Ols peak was negligibly small. Fig. 2. shows the change in the narrow range XPS spectra ([A] ; Cls, [B] ; $Fe2p_{3/2}-2p_{1/2}$ and [C] ; Ols peak) with annealing temperature. It is apparent that both the binding energy and peak intensity of these spectra changed with annealing temperature. The significance of the changes will be discussed later.

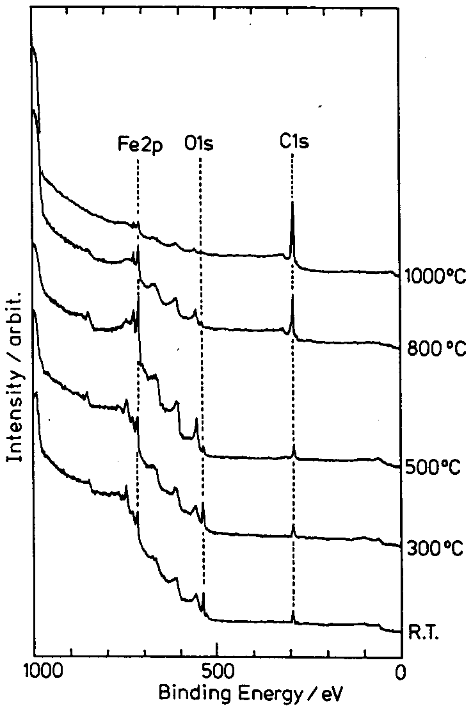

Fig. 1. Changes in the wide range XPS spectra of iron coated graphite with vaccum heatings.

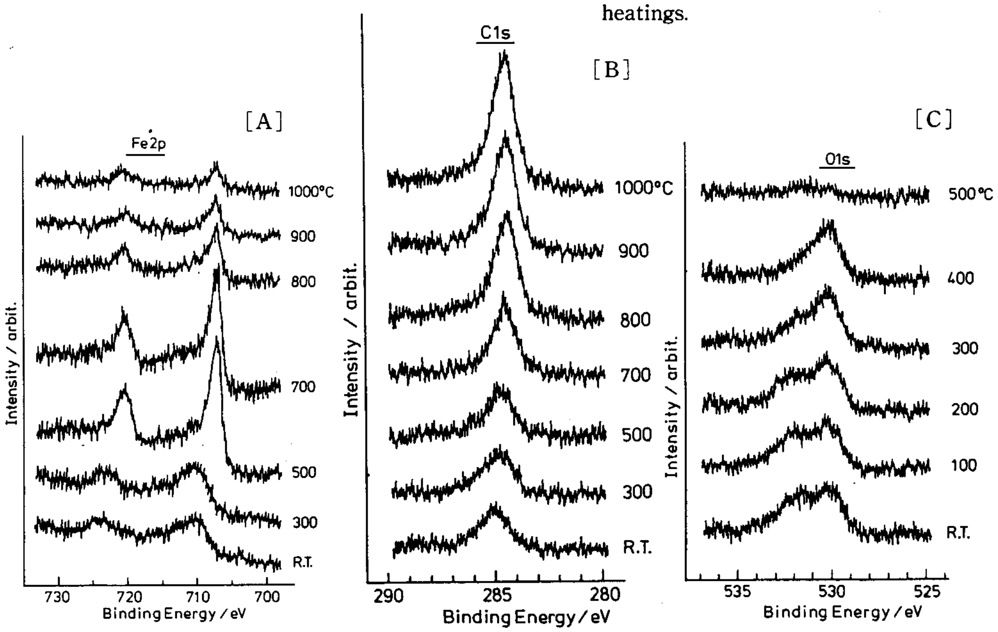

Fig. 2. Change in the narrow range XPS spectra of [A] ; Fe2p, [B] ; Cls and [C] ; Ols peak with vacuum heating.

Fig. 3. shows the change in the surface composition which was determined with use of the relative sensitivity factors of each XPS peak[20]. It is seen in this figure that the surface composition of the iron coated graphite was Fe : O : C=5 : 4 : 1 before the vacuum annealing. At 500℃, however, oxygen disappeared from the surface. At temperatures from 500 to 700℃, the surface composition was kept constant. Above 700℃, the iron concentration gradually decreased, whereas carbon concentration increased with annealing temperature. The surface composition after the annealing at 1000℃ for 10minutes was Fe : C=3 : 97. This value did not change further with additional annealing treatment at 1000℃.

Fig. 4. shows the change in the binding energy of [A] ; Fe2p$_{3/2}$, [B] ; Cls and [C] ; Ols peak. It is seen that the binding energy of Fe2p$_{3/2}$ peak was kept constant at 710.0eV below 500℃. It decreased suddenly to 706.8eV at this temperature and remained at this value till 700℃. At higher temperatures, it increased to 707.0eV.

The Cls peak was initially observed at 285.1eV. It gradually moved toward the lower binding energy side with annealing temperature. Above 800℃, its binding energy was kept costant at 284.3eV.

Two peaks were observed for Ols, indicating the presence of two distinct oxygen species on the surface below 400℃. These peaks, however, disappeared from the surface above 500℃. It was observed

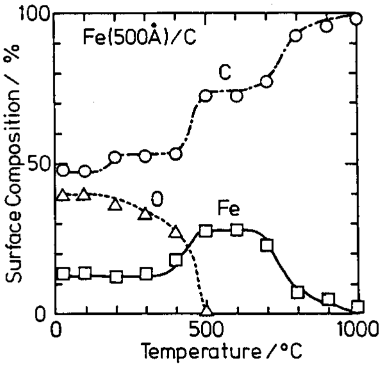

Fig. 3. Change in the surface composition of iron coated graphite with vacuum heating.

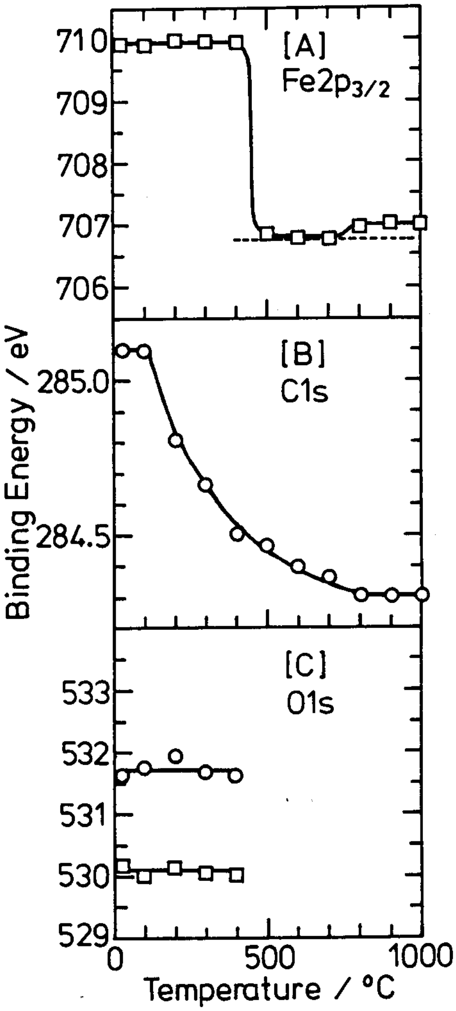

Fig. 4. Change in the binding energy of [A] ; Fe2p$_{3/2}$, [B] ; Cls and [C] ; Ols peak.

that the deuterium ion bombardment on the Fe/Papyex sample did not change the surface composition and binding energy of each peak.

3 - 2 Thermal desorption spectroscopy for hydrogen isotopes

Fig. 5. shows the desorption spectra of D_2 for Fe/Papyex and Papyex. In each of the measurements, the deuterium ion fluence was 1.5×10^{17} ions/cm^2 and the temperature ramp was 2K/sec. The Papyex sample showed a broad spectrum ranging from 750 to 1273K. The TDS for Fe/Papyex differed considerably from that of Papyex : a new and sharp peak appeared at 970K. This is denoted as [Fe/C]-peak in the present study. Contrary to the fact that the TDSs for Papyex become reproducible only after the total amount of ion implantation exceeds 10^{19} ions/cm^2, reproducible TDSs were observed for the Fe/Papyex sample from the beginning of the ion implantation -desorption cycles.

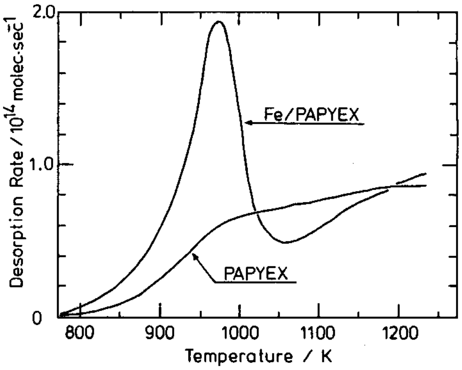

Fig. 5. Desorption spectra of D_2 for Fe/Papyex and Papyex.

Fig. 6. shows the fluence dependence of [Fe/C]-peak. These spectra were measured for the deuterium ion fluence ranging from 1×10^{17} to 3×10^{17} ions/cm^2. After the implantation at room temperature, the sample was heated to 1273K with a temperature ramp of 4K/sec. It is seen that the peak temperature moved to lower temperature side with increasing amount of the implantation.

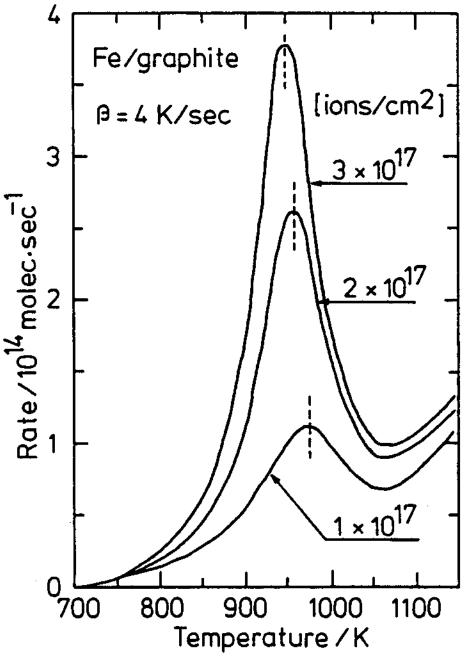

Fig. 6. Fluence dependence of [Fe/C]-peak temperature.

Such fluence dependece of the peak temperature suggests that the rate limiting step for [Fe/C]-peak is not the diffusion process, but surface reaction[12,21,22]. On analogy of the n-th order surface reaction, the peak temperature, T_p, is considered to be a function of activation energy, E_d, frequency factor, ν_d, temperature ramp, β, and concentration of deuterium in the graphite, σ, as

$$(E_d/RT_p^2) = (n\nu_d\sigma^{n-1}/\beta)\exp(-E_d/RT) \tag{1}$$

or rearranging as

$$\ln(T_p^2/\beta) = (E_d/RT_p) + \ln(E_d/n\nu_dR) - (n-1)\ln\sigma \tag{2}$$

Equation (2) indicates that the plots of $\ln(T_p^2/\beta)$ vs. $(1/T_p)$ result in a straight line if the concentration, σ, is kept constant in the series of implantation-desorption measurements. The slope gives the activation energy irrespective to the reaction order.

Fig. 7. shows the plots of $\ln(T_p^2/\beta)$ vs. $(1/T_p)$ for three hydrogen isotopes. In these measurements, the ion fluence was kept constant for each run of a given isotope implantation : 1×10^{16} for H_2, 1×10^{16} for D_2 and 3×10^{15} ions/cm^2 for T_2. The temperature ramp was varied in the range from 2 to 8K/sec. As seen in the figure, those plots resulted in straigt lines. The slopes of those lines were the same for three hydrogen isotopes. That is, no isotope effect was observed on the activation energy for desorption.

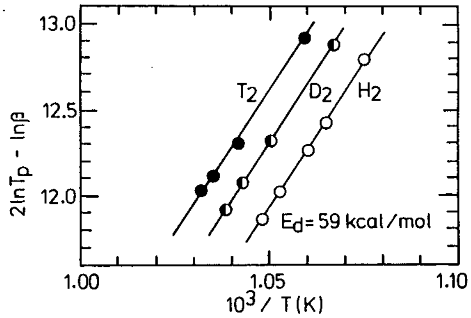

Fig. 7. Plots of $\ln(T_p^2/\beta)$ vs. $(1/T_p)$.

By rearranging eq. (1), the following equation is obtained.

$$\ln(\beta E_d/RT_p^2) + (E_d/RT_p) = (n-1)\ln\sigma + \ln(n\nu_d) \tag{3}$$

This equation indicates that the plots of $\ln(\beta E_d/RT_p^2) + (E_d/RT_p)$ vs. $\ln\sigma$ should result in a straight line, from the slope of which the reaction order, n, is determined. The plots are shown in Fig. 8. It is apparent from the straight line that the reaction order is 2.

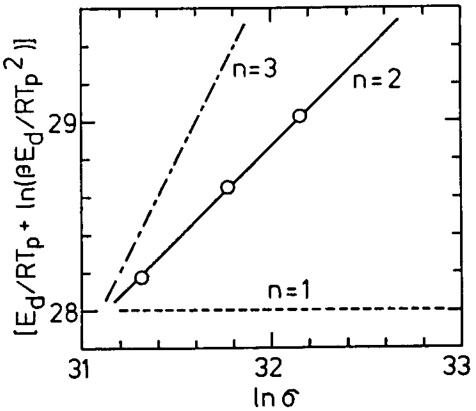

Fig. 8. Plots of $\ln(\beta E_d/RT_p^2) + (E_d/RT_p)$ vs. $\ln\sigma$.

With use of those values, E_d, and n, the frequency factor, ν_d, can be determined from the intersection of the straight lines, shown in Fig. 7 and/or 8, with the ordinate. The kinetic parameters for [Fe/C]-peak thus determined were as follows :

$$k(H_2) = (7\times10^{-4})\exp(-59\times10^3/RT) \quad (4)$$

$$k(D_2) = (4\times10^{-4})\exp(-59\times10^3/RT) \quad (5)$$

$$k(T_2) = (1\times10^{-3})\exp(-59\times10^3/RT) \quad (6)$$

The units of activation energy and frequency factor are [cal/mol] and [l/molec·sec], respectively. The unit of the latter is a consequence that the amount of hydrogen isotope, σ' [atoms], is used in the above eqs. instead of the concentration, σ [atoms/cm^3].

Fig. 9. shows the comparison of the observed [Fe/C]-peaks of three hydrogen isotopes with the calculated peaks using the determined kinetic parameters described by eqs. (4)—(6) in the observed rate equation, $v_d = k\sigma'^2$. All of the calculated spectra for three hydrogen isotopes in different experimental conditions agreed quite well with the observed ones : it is mentioned that both the peak intensity and temperature were reproduced quite well by the simulation.

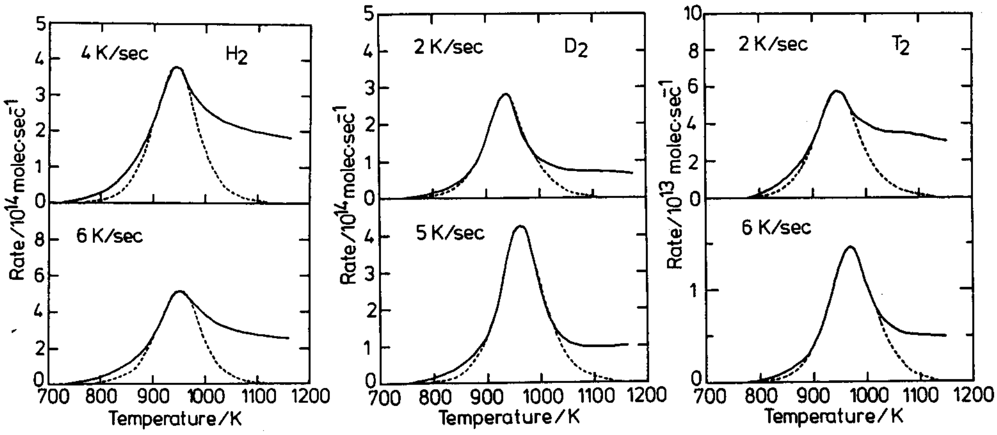

Fig. 9. Comparison of the observed [Fe/C]-peaks of three hydrogen isotopes with the calculated peaks using kinetic parameter described by eqs. (4)—(6).

4 Discussion

4-1 Surface characterization of Papyex doped with iron

On the surface of Papyex coated with iron film, a relatively large amount of oxygen and carbon was detected. This is because the sample was exposed to air in order to remove it from the sputtering apparatus to the other UHV system with XPS-SIMS optics. The binding energy of $Fe2p_{3/2}$ and spin-orbit splitting width were 710.0 and 13.6ev, respectively. One of the Ols peak was observed 530.1eV. With reference to the reported values for these peaks, it is apparent that iron was present on this surface as iron oxide such as Fe_2O_3[20]. In addition, the Cls peak observed on this surface

(285.1eV) was somewhat higher than that observed for graphite (284.5eV). This fact and the appearance of the Ols peak at 531.6eV suggests that carbon was present on the surface as graphite and adsorbed species such as CO[20,23]. The presence of graphite on this surface is considered due to island and/or crack structure of the iron film.

With respect to the shift of the Fe2p$_{3/2}$ peak from 710.0 to 707.0eV with annealing at 500℃, it is considered that the iron oxide converted to metallic state at this temperature. This explanation is consistent with the fact that the Ols peak disappeared and the Cls peak shifted to the lower binding energy side. The change in the surface state, therefore, will be described as follows :

$$Fe_2O_3 + 3C\,(\text{contaminant/graphite}) \rightleftharpoons 2Fe + 3CO \qquad (7)$$

$$(3Fe_2O_3 + C \rightleftharpoons 2Fe_3O_4 + CO) \qquad (7\text{-}1)$$

$$(Fe_3O_4 + C \rightleftharpoons 3FeO + CO) \qquad (7\text{-}2)$$

$$(FeO + C \rightleftharpoons Fe + CO) \qquad (7\text{-}3)$$

$$(Fe_3O_4 + 4C \rightleftharpoons 3Fe + 4CO) \qquad (7\text{-}4)$$

$$Fe_2O_3 + 3CO \rightleftharpoons 2Fe + 3CO_2 \qquad (8)$$

$$(3Fe_2O_3 + CO \rightleftharpoons 2Fe_3O_4 + CO_2) \qquad (8\text{-}1)$$

$$(Fe_3O_4 + CO \rightleftharpoons 3FeO + CO_2) \qquad (8\text{-}2)$$

$$(Fe_3O_4 + 4CO \rightleftharpoons 3Fe + 4CO_2) \qquad (8\text{-}3)$$

$$(FeO + CO \rightleftharpoons Fe + CO_2) \qquad (8\text{-}4)$$

The free energy change in the reduction of the iron oxide by carbon, eq. (7), and that by carbon monoxide, eq. (8), are negative above 500℃[24]. Besides, a part of the adsorbed CO is considered to be desorbed from the surface.

At higher temperatures above 800℃, the Fe2p$_{3/2}$ peak shifted up to 0.2eV. On account of the fact that binding energy of Fe2p$_{3/2}$ of iron carbide such as Fe_3C is 0.2 eV higher than that of metallic iron[25], whereas the binding energy of Cls of the carbide is 0.3eV lower than that of graphite, the change in the surface state at this temperature will be described as

$$3Fe + C\,(\text{graphite}) \rightleftharpoons Fe_3C \qquad (9)$$

The free energy change in this reaction becomes negative above 800 to 900℃[26].

4-2 Effect of iron dopant on the desorption process

The TDSs of deuterium for Fe/Papyex differed considerably from those for Papyex. This is apparently due to the presence of iron dopant, amounting only 3 at.%. The analysis of [Fe/C]-peak revealed that the desorption obeys the second order kinetics with respect to the concentration of hydrogen atoms in the sample, indicating that the rate determining step for desorption is the recombination reaction of hydrogen atoms on the surface. This conclusion is also valid for other hydrogen isotepes.

The activation energy of the desorption forming [Fe/C]-peak was determined as 59kcal/mol for three isotopes. That is, the isotope effect on this term is negligibly small. On the other hand, the frequency factors differed from each other among three isotopes. The difference on this term between hydrogen and deuterium is apparently due to the isotope effect. On the other hand, there is some doubt about the frequency factor for tritium, because its value appears too large in comparison with those for the other two. In addition, the purity of the tritium gas used in the present study was rather poor in comparison with those of hydrogen and deuterium. The effect of the impurity gases such as H_2, CO and H_2O should be taken into account. This calls for the re-examination of the frequency factor for tritium by use of pure tritium gas in future.

Contrary to the TDSs of hydrogen isotopes for graphite, the TDSs for Fe/Papyex were reproduced quite well from the beginning of the ion implantation-desorption cycles. It indicates that the damage modification as observed for pure graphite(12,13) does not play an important role for the desorption process of hydrogen isotopes implanted into this sample. This means that the change in TDSs for Fe/Papyex from those for Papyex are not due to the accumulation of radiation damage, but a consequence of the presence of iron dopant.

We have found that the TDSs of hydrogen isotopes for graphite modified with accumulation of radiation damage consist of three desorption peaks(12,27,28) : being denoted as Peak [I], [II] and [III] from the lower temperature side. Peak [I] corresponds to the desorption of hydrogen atoms trapped on normal graphite lattice and Peak [II] results from the desorption from damaged region in the graphite. In the present study, it was found that the kinetic parameters for [Fe/C]-peak agreed quite well with those of Peak [II] observed for the graphite with damage modification(29,30)*1. Namely, Peak [I] disappeared from the TDSs for Fe/Papyex. The disappearance is considered to be due to (1) the disappearance of the normal graphite lattice, (2) the reduction of trapping ability of the normal graphite lattice for hydrogen atoms, and/or (3) the impediment of recombination of hydrogen atoms on the normal graphite lattice, as a result of the presence of iron.

---

*1 According to separate experiments having been done recently, Peak [III] is ascribed to diffusion controlled process(31).

As mentioned above, the desorption mechanism and kinetic parameters for [Fe/C]-peak agreed quite well with those for Peak [II] for pure graphite modified with radiation damage. Namely, [Fe/C]-peak is identical with Peak [II]. This is explained as follows. The binding energy of the Cls peak for Fe/Papyex was 0.2eV lower than that of the normal graphite. The shift of 0.2eV to lower binding energy side has been also observed for the graphite modified with radiation damage[10,11]. Such shift of the Cls peak indicates that electronic charge on carbon increases with the presence of radiation damage and/or iron dopant. From the viewpoint of the change in the electronic state of carbon, they are the same. Consequently, it is considered that the appearance of Peak [II] and [Fe/C]-peak is due to the change in the electronic state of carbon, irrespective to its cause.

4-3 Surface recombination factor for [Fe/C]-peak

The surface recombination factor of hydrogen atoms, k_r [cm^4/molec · sec], and pseudo surface recombination factor, k_sK^2 [cm^2/molec · sec],are defined as below[32,33], respectively.

$$N(t) = k_r C^2 \tag{10}$$

$$k_s K^2 = (N_b/N_s)^2 k_r \tag{11}$$

where N(t) is the desorption rate of hydrogen [molec/cm^2 · sec] and C is the concentration of hydrogen atoms in the sub-surface region [molec/cm^3]. N_s and N_b are the densities of the trapping sites on the surface and sub-surface layer, respectively. We have determined the recombination factors of three hydrogen isotope atoms for Peak [I][33]. Following the same procedures as Peak [I], those for [Fe/C]-peak were estimated as

$$k_r(H_2) = (1.5\times10^{-15})\exp(-59\times10^3/RT)\ [cm^4/\text{molec}\cdot\text{sec}]$$
$$k_r(D_2) = (9.6\times10^{-15})\exp(-59\times10^3/RT)$$
$$k_r(T_2) = \nu_d(T_2)\times(2.6\times10^{-12})\exp(-59\times10^3/RT)$$

$$k_sK^2(H_2) = (5.44)\exp(-59\times10^3/RT)\ [cm^2/\text{molec}\cdot\text{sec}]$$
$$k_sK^2(D_2) = (3.44)\exp(-59\times10^3/RT)$$
$$k_sK^2(T_2) = \nu_d(T_2)\times(9.4\times10^3)\exp(-59\times10^3/RT)$$

These results are shown in Fig. 10, where the recombination factors for Peak [I] are also shown for the sake of comparison[33]. It should be mentioned here that the results for Peak [II] are essentially identical with those for [Fe/C]-peak. It is seen in the figure that the recombination factor for [Fe/C]-peak is smaller than that for Peak [I] below 500℃. It indicates that the tritium inventory becomes larger with iron doping below 500℃.

According to the observations by Gimzewski et al[17]., the deposition of metallic impurities will amount to over 1×10^{15} atoms/cm^2 in 100 shots of plasma discharge in tokamaks. This fact and the present observations suggest that the physicochemical properties of the graphite first wall will be greatly altered from those of pure graphite with the accumulation of metallic impurities. Namely, the recycling and/or inventory of fuel particles as well as other phenomena such as chemical sputtering will be influenced (being improved or debased) with the presence of metallic impurities on the graphite first wall.

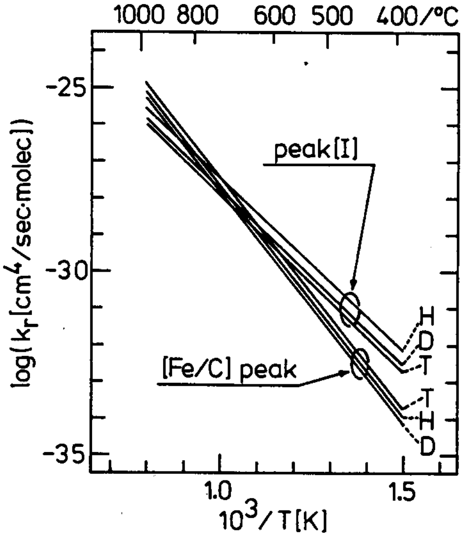

Fig. 10. Comparison of recombination factor, K_r, for [Fe/C]-peak with that for Peak [I].
The data for Peak [I] are taken from ref. [33].

5 Conclusions

Based on the above observations and discussion, we conclude as follows :

(1) Iron deposited on graphite surface combines with carbon to form Fe_3C above 800℃.

(2) Electronic charge on carbon increases owing to the presence of iron of only 3 at. %.

(3) This surface is stable against hydrogen ion bombardment amounting to the fluence over 1×10^{19} ions/cm^2.

(4) The thermal desorption spectra change considerably with the presence of iron from those for pure graphite. This is due to the increase in the electronic charge on carbon.

(5) The desorption spectra for Fe/Papyex lack Peak [I] observed for pure graphite and show sharp and intense [Fe/C]-peak.

(6) The rate limiting step for [Fe/C]-peak is the surface recombination of the trapped hydrogen atoms and the kinetic parameters agree quite well with those for Peak [II] of pure graphite. Namely, [Fe/C]-peak is identical with Peak [II].

(7) The observed kinetic parameters and estimated recombination factors are as follows :

$$k(H_2) = (7\times10^{-4})\exp(-59\times10^3/RT)\ [1/\mathrm{molec}\cdot\mathrm{sec}]$$
$$k(D_2) = (4\times10^{-4})\exp(-59\times10^3/RT)$$
$$k(T_2) = \nu_d(T_2)\exp(-59\times10^3/RT)$$

$$k_r(H_2) = (1.5\times10^{-15})\exp(-59\times10^3/RT)\ [\mathrm{cm}^4/\mathrm{molec}\cdot\mathrm{sec}]$$
$$k_r(D_2) = (9.6\times10^{-15})\exp(-59\times10^3/RT)$$
$$k_r(T_2) = \nu_d(T_2)\times(2.6\times10^{-12})\exp(-59\times ao^3/RT)$$

$$k_sK^2(H_2) = (5.44)\exp(-59\times10^3/RT)\ [\mathrm{cm}^2/\mathrm{molec}\cdot\mathrm{sec}]$$
$$k_sK^2(D_2) = (3.44)\exp(-59\times10^3/RT)$$
$$k_sK^2(T_2) = \nu_d'(T_2)\times(9.4\times10^3)\exp(-59\times10^3/RT)$$

Acknowledgements

The authors gratefully acknowledge to Dr. K. Sone of Japan Atomic Energy Research Institute for providing us the Papyex sample. The acknowledgement is also due to Prof. K. Mori of Toyama University for iron coating on Papyex.

This work was supported by a Grant-in-Aid for Fusion Research under Special Research Program from the Ministry of Education, Science and Culture of Japan.

References

1) R. Yamada, K. Nakamura, K. Sone and M. Saidoh, J. Nucl. Mater., **95** (1980) 278.
2) R. Yamada, K. Nakamura and M. Saidoh, ibid., **111/112** (1981) 167.
3) V. Philipps, K. Flaskamp and E. Vietzke, ibid., **111/112** (1982) 781.
4) J. Roth, J. Bohdansky and K. L. Wilson, ibid., **111/112** (1982) 775.
5) J. Roth, J. B. Roberto and K. L. Wilson, ibid., **122/123** (1984) 1447.
6) P. Hucks, K. Flaskamp and E. Vietzke, ibid., **93/94** (1980) 558.
7) W. R. Wampler, D. K. Brice and C. W. Magee, ibid., **63** (1976) 415.
8) J. Roth, B. M. U. Scherzer, R. S. Blewer, D. K. Brice, S. T. Picraux and W. R. Wampler, ibid., **93/94** (1980) 601.
9) K. Sone and G. M. McCracken, ibid., **111/112** (1982) 606.
10) K. Ashida, K. Ichimura, M. Matsuyama, H. Miyake and K. Watanabe, ibid., **111/112** (1982) 769.
11) K. Ashida, K. Ichimura and K. Watanabe, J. Vac. Sci. Technol., **A1** (1983) 1465.

12) K. Ashida, K. Ichimura, M. Matsuyama and K. Watanabe, J. Nucl. Mater., **128/129** (1984) 792.

13) K. Ashida, K. Kanamori, K. Ichimura, M. Matsuyama and K. Watanabe, ibid., **137** (1986) 288.

14) E. Taglauer, ibid., **128/129** (1984) 141.

15) B. Emmoth, M. Braun, H. E. Satherblom, P. Wienhold, J. Winter and F. Waelbrock, ibid., **128/129** (1984) 195.

16) H. Wolff, H. Grote, D. Hildebrandt, M. Laux, P. Pech, C. D. Reiner and H. Strusny, ibid., **128/129** (1984) 219.

17) J. K. Gimzewski, S. Veprek, F. Hofmann, Ch. Hollenstein, J. B. Lister, A. Pochelon and P. Groner, J. Vac. Sci. Technol., **A4** (1986) 90.

18) V. I. Nefedov, Ya, Saiyn, G. Leonhardt and R. Sheibe, J. Electron Spect. Relat. Phonom., **10** (1977) 121.

19) K. Watanabe, H. Miyake and M. Matsuyama, J. Vac. Sci. Technol., in press.

20) C. D. Wagner, W. M. Riggs, L. E. Davis, J. F. Mouler, and G. E. Muilenberg, "Handbook of X-ray Photoelectron Spectroscopy" (Perkin-Elmer, Eden Prairie, M. N. 1979).

21) P. A. Redhead, Vacuum, **12** (1962) 203.

22) K. Ichimura, N. Inoue, K. Watanabe and T. Takeuchi, J. Vac. Sci. Technol., **A2** (1984) 1341.

23) P. R. Norton, Surface Sci., **44** (1974) 624.

24) "Kinzoku Binran", (Maruzen, 1971) p.299-303.

25) I. N. Shabanova and V. A. Trapeznikov, J. Electron Spect. and Relat. Phenom., **6** (1975) 297.

26) "Kinzoku Databook", (Maruzen, 1974) p,84.

27) K. Ashida, K. Ichimura and K. Watanabe, J. Vac, Soc. Jpn., **26** (1983) 397 (in Japanese).

28) K. Ashida, K. Ichimura and K. Watanabe, ibid., **29** (1986) 369 (in Japanese).

29) K. Ashida, K. Ichimura, M. Matsuyama and K. Watanabe, J. Nucl. Mater., in press.

30) K. Ashida, K. Ichimura and K. Watanabe, J. Vac. Soc. Jpn., in press (in Japanese).

31) K. Ashida, M. Matsuyama and K. Watanabe, Ann. Rept. Tritium Res. Centr, **6** (1986) 27 (in Japanese).

32) R. A. Langley, J. Nucl., Mater., **128/129** (1984) 622.

33) K. Watanabe and K. Ashida, Ann. Rept. Tritium Res. Centr, **5** (1985) 41.